Enhancement of Tumor-to-Nontumor Localization Ratios by Hepatocyte-Directed Blood Clearance of Antibodies Labeled with Certain Residualizing Radiolabels

Sagar Patel, Rhona Stein, Gaik Lin Ong, David M. Goldenberg and M. Jules Mattes

Garden State Cancer Center at the Center for Molecular Medicine and Immunology, Belleville, New Jersey

To increase tumor-to-nontumor localization ratios of injected radiolabeled antibodies (Abs), several interrelated methods were used. **Methods:** The model systems used were two human carcinoma xenografts grown in nude mice, targeted by antibodies RS11 (antiepithelial glycoprotein-2) or MN-14 (anticarcinoembryonic antigen). The Abs were conjugated with biotin and ^{111}In-benzyl diethylenetriamine pentaacetic acid, and, at various times after injection, were cleared by intraperitoneal injection of galactosylated streptavidin, which delivers the complexes to hepatocytes. The radiolabel used was selected because it is retained within tumors after catabolism of the Ab by the tumor cell but is quite rapidly excreted from hepatocytes into bile. **Results:** With blood clearance induced at 24 h, and dissection 5 h later, high tumor-to-nontumor ratios were attained. Depending on the model used, tumor-to-blood ratios were 16:1 to 31:1, and tumor-to-nontumor ratios for the kidney, lungs and bone were also high and greatly increased by the clearance regimen. Despite clearance into the liver, tumor-to-liver ratios remained >1, due to fairly rapid biliary excretion of the label. The absolute antibody uptake by the tumors was also high, because 24 h was allowed for the Ab to penetrate and bind to cells within the subcutaneous tumors. **Conclusion:** The method described produced high tumor-to-nontumor ratios at 1 d after injection and may be advantageous for tumor imaging with antibodies. Radiation dosimetry calculations indicate that there is only a slight advantage with this approach for radioimmunotherapy.

Key Words: antibody conjugates; tumor imaging; ^{111}In-diethylenetriamine pentaacetic acid antibody conjugates

J Nucl Med 1999; 40:1392–1401

Radiolabeled antibodies (Abs) are increasingly being used for imaging and therapy of tumors and other diseases (*1*). A basic goal is to obtain high tumor-to-nontumor ratios of the injected label. One of the inherent obstacles is the fact that Abs normally have very long circulation times, longer than that of any other major serum protein (*2*), which means that serum levels, and hence levels in all normal tissues, will be relatively high. This will limit the tumor-to-nontumor ratios, even if very high Ab uptake in the target tissue is achieved. Many approaches have been used to circumvent this problem. One approach is to use a modified Ab that is cleared more rapidly from the blood, such as a Fab′ or $F(ab')_2$ Ab fragment. Although the use of Ab fragments has produced successful clinical imaging within 24 h (*3*), this approach inevitably results in lower tumor uptake, due primarily to the much faster blood clearance. The use of Ab fragments also results in high kidney uptake (*4*). A second strategy is to rapidly clear the circulating Ab from the blood at a desired time, approximately 2 d postinjection, after the tumor has been thoroughly penetrated. This approach is particularly attractive if large amounts of Ab are injected and the antigen on the tumor becomes saturated, because, at that point, excess circulating Ab is clearly a disadvantage.

Conceptually, the simplest mode of blood clearance is extracorporeal immunoadsorption (*5*). However, this approach seems cumbersome and is unlikely to clear Ab from the blood as completely as methods in which a clearing agent is injected. Rapid clearance in vivo has been induced by various mechanisms (*6–8*). However, two basic problems have made it difficult to use this strategy effectively. First, it has been found that after Ab is cleared from the blood, radioactivity in the tumor decreases substantially (*5–9*). Second, the cleared Ab usually goes to the liver, resulting in high uptake in this organ (*5–7*). We now have developed strategies to deal with both of these problems.

The loss of radioactivity from the tumor after rapid blood clearance has several distinct causes, which will be of varying importance depending on the particular Ab and tumor, but a significant part is due to catabolism of the Ab and release of catabolites. Conventional iodine-labeled catabolites are released rapidly from the cells. However, ^{111}In-labeled catabolites and certain iodine labels are trapped within cells, probably within lysosomes (*10,11*). The use of such labels, termed residualizing radiolabels, can provide a major advantage in some circumstances (*11,12*). Residualizing labels, however, are trapped not only in tumor cells or other target cells, but also in any other organ that normally

Received Nov. 2, 1998; revision accepted Jan. 13, 1999.

For correspondence or reprints contact: M. Jules Mattes, PhD, Center for Molecular Medicine and Immunology, 520 Belleville Ave., Belleville, NJ 07109.

catabolizes the Ab, primarily the liver, spleen and kidney (*11*). The problem of retention in normal tissues is markedly increased when clearance mechanisms are used, because activity going to the liver, for example, would be expected to be trapped there for long periods, as has been reported (*6,7*).

To reduce the presence of radioactivity in the liver, we have taken advantage of the fact that the hepatocyte is the only cell in the body that can deliver metabolic products directly to the bile for excretion. There is evidence that the indigestible material present in aged lysosomes in hepatocytes can be directly delivered, through exocytosis, into the bile (*13,14*). Thus, there is a basis to speculate that residualizing labels may be trapped in the lysosomes of tumor cells but may be efficiently excreted by hepatocytes. The first data supporting this idea were described by Arano et al. (*15*) in their investigation of the liver catabolism of various radiolabels. They examined radiometals, conjugated to albumin, delivered to either hepatocytes (through the asialoglycoprotein receptor) or Kupffer cells (through the mannose receptor). Their results demonstrated that ^{111}In-benzyl-ethylenediaminetetraacetic acid (EDTA), but not ^{111}In-diethylenetriamine pentaacetic acid (DTPA) (prepared from the cyclic anhydride), was excreted much more rapidly from hepatocytes than from Kupffer cells, and that excretion was through bile. In this context, Kupffer cells can be considered similar to tumor cells, in that neither has direct entry into the biliary system. These studies provided the first clear evidence for a label with the desired properties, namely, ^{111}In-benzyl-EDTA. Our previous studies demonstrated that ^{111}In-benzyl-DTPA also is rapidly excreted from hepatocytes into bile, although it is retained within tumor cells and therefore is another appropriate label for this approach (*16*). It was interesting that ^{125}I-iodo-dilactitol-tyramine (DLT), another residualizing label, was not processed like ^{111}In-benzyl-DTPA by hepatocytes, although otherwise these are very similar residualizing labels. The last requirement to use this strategy was a method to induce blood clearance into hepatocytes at any time desired. We use herein a galactosylated clearing agent, namely, galactosylated-streptavidin (gal-SA) in conjunction with biotinylated Abs, which delivers complexes to the asialoglycoprotein receptor (ASGP-r).

MATERIALS AND METHODS

Tumor Cell Lines and Growth of Xenografts

The cell lines and their growth conditions were previously described (*4,11*). Calu-3 lung carcinoma cells were propagated in vitro, and 10^7 tissue culture cells were injected subcutaneously into nude mice. LS174T colon carcinoma cells were serially transplanted in nude mice.

Antibodies, Radiolabeling and Biotinylation

The Abs used, all mouse IgG1s, were described previously. For Calu-3 tumors, the Ab used was RS11 (antiepithelial glycoprotein-2 [EGP-2]) (*11*). Another Ab to EGP-2, MJ37 (*17*), was used in some of the earlier experiments. The antigen EGP-2 is recognized by many widely used monoclonal Abs (mAbs), including 17-1A, KS1/4 and NRLU-10 (*17*). For LS174T tumors, the Ab was MN-14 (anticarcinoembryonic antigen [anti-CEA]) (*4*). Labeling with conventional iodine, using chloramine T, was described previously (*11*), and streptavidin was iodinated by similar methods. The method of biotinylating Abs, using NHS-LC-biotin (Pierce Chemical Co., Rockford, IL) has been described (*18*), and produced 7–12 biotins per IgG. Biotinylation was performed before 4-isothiocyanato-benzyl-DTPA conjugation and did not noticeably interfere with DTPA conjugation, although some of the amino groups were blocked. The DTPA/Ab molar ratios were 1–2, and 0.1 mg of Ab was labeled with 37 MBq ^{111}In, as described (*11*). Briefly, the $^{111}InCl_3$ was diluted with 3 volumes of 0.5 mol/L ammonium acetate, pH 5.5, then mixed with the Ab. After 1 h at room temperature, excess DTPA was added to a final concentration of 1 mmol/L, and 15 min later the volume was made up to 0.5 mL with phosphate-buffered saline (PBS) containing 1.0% human serum albumin. All labeled preparations were analyzed by instant thin-layer chromatography on Silica gel strips (No. 61885; Gelman Sciences, Ann Arbor, MI). The developing buffers were acetone, for iodinated proteins, and 10 mmol/L EDTA for ^{111}In-labeled proteins. Representative preparations were also analyzed by gel filtration high-performance liquid chromatography on a Bio-Sil SEC-250 column (BIO-RAD, Hercules, CA), with a running buffer of PBS. More than 90% of the radioactivity migrated as expected for intact IgG (usually >95%). Immunoreactivity was monitored by two types of cell-binding assays: use of a large number of cells (antigen excess) to demonstrate the maximum bindable counts per minute (*11*); and use of fewer cells and nonsaturating Ab concentrations to provide an indication of Ab avidity (*19*). The Ab conjugates prepared for these experiments had fully intact immunoreactivity, in comparison with Abs labeled by simpler and more conventional methods (iodination or ^{111}In-benzyl-DTPA without additional biotin).

Use of Galactosylated Streptavidin as a Clearing Agent

The methods described by Marshall et al. (*9*) were followed, with slight modifications. Streptavidin (Vector Labs, Burlingame, CA) was galactosylated with cyanomethyl-tetra-O-acetyl-1-thio-β-D-galactopyranoside (*20*). At 1–2 d after 0.19–0.37 MBq injection of the radiolabeled, biotinylated Ab, 40 μg gal-SA was injected, either intraperitoneally or intravenously, and the blood clearance of the Ab was monitored by bleeding repeatedly from the tail vein. The preliminary experiments were performed with normal outbred mice (strain ICR; Taconic Labs, Germantown, NY). The variations in this protocol that were tested are described in the results section. The final method developed, used in the biodistribution experiments, was to inject 40 μg gal-SA intraperitoneally in 0.5 mL, and to similarly inject a second dose of 20 μg gal-SA 3 h later.

Antibody Biodistribution

The general methods used were described previously (*11*). The size of tumors used for biodistribution experiments was 0.13–0.5 g at the time of injection, and groups of 5 mice were used. Various intervals between Ab injection and clearance induction were tested, namely, 17, 24 and 48 h, to determine the interval that was optimal for imaging or therapy (the optimal interval was different depending on the purpose). Mice were dissected at various times, and tissues counted for radioactivity. To show clearly the effect of induced clearance, groups of mice were always killed just before induction of clearance, and 2 h after the second injection of the clearing agent, when blood clearance was essentially complete. The other time points that were included routinely were day 1, 3 and 7 after clearance induction. In addition, most experiments

included a second time point before clearance induction, usually at 4 h; this time point was necessary to allow extrapolation of the curve of uptake/time to time 0. Although experiments with nonreactive control Abs were not included in this study, previous experiments had compared these same specific Abs with nonreactive Abs of the same subclass and demonstrated that Ab localization was predominantly antigen-specific (*11,21*). Statistical comparisons of groups were by Student *t* test.

Dosimetry

Radiation dose estimates delivered to the tumor and normal tissues were calculated from the biodistribution data, as described previously (*11*). Briefly, a graph of percentage injected dose per gram (%ID/g) of tissue versus time was integrated to provide the cumulative disintegrations per gram of tissue per millicurie injected. Because of the induced blood clearance, the rate of loss of radioactivity from normal tissues could not be approximated by a simple exponential curve, and the area under the curve was determined by the trapezoidal method for regions between the data points. For regions before or after the data points, exponential extrapolations were made for the normal tissues, as described previously (*6*), based on either the first two or the last two data points, respectively. Tumor dosimetry was calculated similarly, except that the value at time 0 was set at 0; this conservative assumption will tend to underestimate slightly the dose to the tumor relative to the normal tissues. The S values used to calculate rad doses were based on small sphere models of mouse organs (*22*), which do not assume 100% absorbtion of β-particles. For the blood, the absorbed dose was calculated for a sphere the size of the total blood volume of the mouse (assumed to be 7.4% of the body weight). This is not implied to be an accurate model of the blood, but is useful in that the blood dose calculated has been found to correlate well with experimentally determined bone marrow toxicity, which is the dose-limiting toxicity (*23*).

RESULTS

Effect of Galactosylation on Blood Clearance of Streptavidin

Preliminary experiments investigated the clearance rate of gal-SA, in comparison to the unmodified SA, using iodinated SA. Although unmodified SA was cleared from the blood of mice with a $t_{1/2}$ of approximately 3–4 h, gal-SA was cleared much faster (Fig. 1). By 20 min, virtually all the label was cleared from the blood. At 5 min after injection, substantial activity was still present in the blood, so it can be concluded that complete clearance required approximately 10–20 min. This very rapid clearance is expected for ligands binding to the hepatocyte ASGP-r (*20*) and is consistent with the results of Marshall et al. (*9*). To confirm that clearance was through the ASGP-r, some mice were injected with asialobovine submaxillary mucin intraperitoneally before injection of the radiolabeled gal-SA, as described in previous experiments (*20*). Clearance was effectively inhibited (data not shown).

Use of Galactosylated Streptavidin as a Clearing Agent, in Conjunction with Biotinylated, Radiolabeled Antibody

In preliminary experiments, nontumor-bearing mice were injected intraperitoneally with gal-SA 24 h after intravenous injection of ^{125}I-biotin-Ab MJ37. At 15 min after injection,

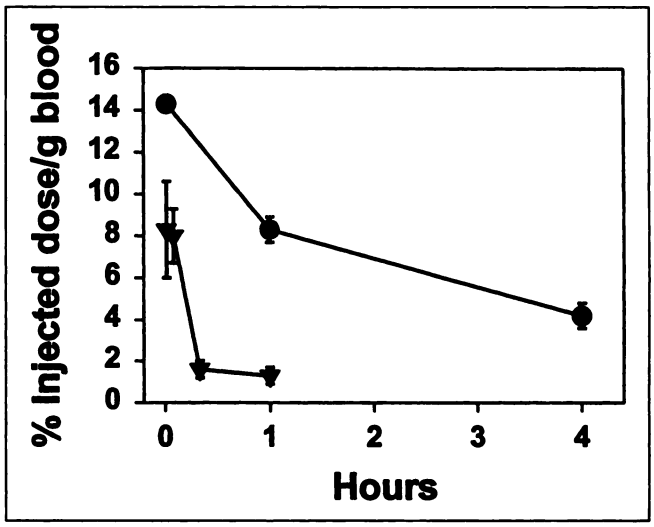

FIGURE 1. Effect of galactose conjugation on blood clearance of SA in normal mice. Blood concentration of SA (●) and gal-SA (▼) at various times after intravenous injection is shown. Values shown are mean ± SD from triplicate mice.

there was very little clearance, but clearance was near-complete at 45 min and complete at 90 min. The change in blood level over this 90-min period was from 11.5 ± 1.1 %ID/g to 1.8 ± 0.1 %ID/g. Additional experiments were performed with an intravenous injection of the gal-SA for comparison. In this case, as expected, the clearance was faster, being complete at 15 min. With the intravenous injection, but not with the intraperitoneal injection, there was a small but distinct rise in the Ab concentration in the blood after the initial clearance (data not shown). The blood level rose from 1.73 ± 0.3 %ID/g at 15 min to 2.64 ± 0.76 %ID/g at 45 min, a 53% rise in the blood concentration that was statistically significant ($P < 0.05$). To obtain a more complete clearance, two intraperitoneal injections of gal-SA were administered, separated by a 3-h interval. The second injection produced an approximately two-fold decrease in the blood concentration, from 1.65 ± 0.27 %ID/g (just before the injection), to 0.85 ± 0.17 %ID/g, (at 1 h after the injection). Although this absolute difference appears small, it would result in an approximately two-fold improvement in the tumor-to-blood ratio. Therefore, the use of two intraperitoneal injections, with a first dose of 40 μg, followed 3 h later by a second dose of 20 μg, was adopted as our standard clearance method. Results obtained using this protocol are shown in Figure 2. The decrease in Ab concentration in the blood was approximately 10-fold.

Enhancement of Tumor-to-Nontumor Ratios in Nude Mice Bearing Human Tumor Xenografts

The strategy described was applied initially to a model using the lung carcinoma Calu-3 and the Ab RS11 (anti-EGP-2), with clearance at 24 h. Figure 3 shows the %ID/g and the tumor-to-nontumor ratios at various times. Figure 3 includes a magnification showing only the two time points that were just before clearance, at 24 h and just after

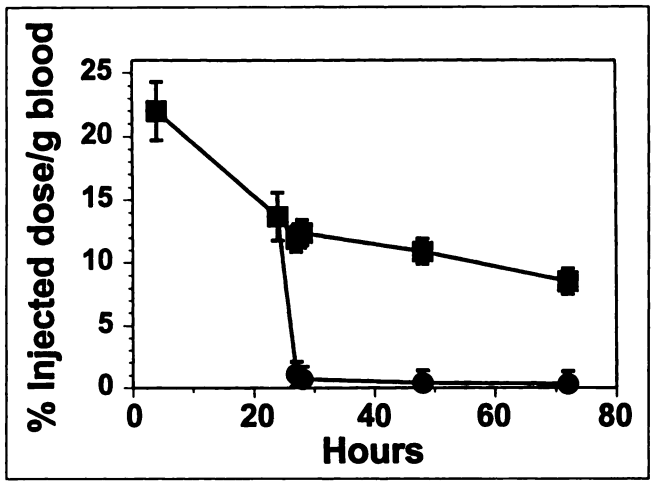

FIGURE 2. Delayed rapid blood clearance of ^{125}I-biotinylated-MJ37 induced by injection of gal-SA (●). Mice were given two intraperitoneal injections of gal-SA at 24 h (immediately after 24-h bleeding) and at 27 h (immediately after 27-h bleeding), using dose of 40 μg and 20 μg/mouse, respectively. Blood clearance rate in control mice, not injected with gal-SA, is also shown (■). Mean ± SD are shown. Second dose of gal-SA produced small but significant decrease in level of circulating Ab, although not clearly evident in this figure.

clearance (5 h later), which is necessary because these two points are too close together to show up clearly in the complete figure. Blood clearance was effective, with a reduction from 14.1 ± 1.5 %ID/g at 24 h to 2.2 ± 0.9 %ID/g at 29 h, a 6.4-fold decrease. Clearance from the other normal tissues was not as effective as clearance from the blood, presumably because of the content of interstitial fluid in these tissues, but the lung and kidney had a high clearance factor of approximately 3.5-fold. In contrast, radioactivity in the tumor was retained quite well, with only an 8.4% decrease, so the tumor-to-nontumor ratios increased markedly for most normal tissues. The tumor-to-blood ratio increased from 2.4 ± 0.7 at 24 h to 16.0 ± 11.3 at 29 h. At the same time points, the tumor-to-kidney ratio increased from 7.2 ± 2.2 to 23.2 ± 12.0, and the tumor-to-lung ratio increased from 4.8 ± 2.1 to 14.4 ± 2.8. The spleen and bone showed considerable benefit from induced clearance, although not as great as the kidney and lungs. The muscle was not significantly affected by the blood clearance, because the percentage of the injected dose per gram muscle did not change substantially as a result of blood clearance, presumably reflecting the low content of blood in the muscle. However, tumor-to-muscle ratios were very high in any case, even in the absence of induced blood clearance of the Ab.

There were two normal tissues in which the isotope accumulated because of clearance. One, of course, was the liver, because clearance was into the liver, and because biliary excretion requires some time. However, tumor-to-liver ratios were >1 at all time points, which means that excretion from the liver was quite fast and that the radioactivity cleared into the liver did not remain there for long. The other site of normal tissue uptake was in the intestines, both large and small, but particularly in the large intestine; however, this uptake was transient. It is important to note that the entire large and small intestines (including their contents) were collected and counted, so this uptake can be attributed to biliary excretion, as seen previously in similar experiments, in which fecal excretion was assayed (*16*). This accumulation in the intestines was totally eliminated by 72 h (the next time point in these experiments), at which time the tumor-to-nontumor ratios for the intestines were as high as for the highest normal tissues (muscle and bone), in the range of 25:1–40:1.

Table 1 provides a comparison of these results with those of previous localization experiments that used a similar label, ^{88}Y-benzyl-DTPA, on the same Ab and with the same Calu-3 tumor. The tumor sizes were similar. In this earlier experiment, the labeled Ab was simply injected, and biodistribution monitored at various times. The difference between the radiometals used, ^{88}Y versus ^{111}In, is not significant, because the only significant difference in biodistribution between these two labels (with the benzyl-DTPA chelate used) is a slight uptake of ^{88}Y in washed bone (*24*). We note that the data in Table 1, for the gal-SA clearance method, represent means of data from two experiments, one of which was described in detail in Figure 3; therefore, the values are slightly different from those in that figure. As shown, there are two key advantages of the gal-SA clearance method: higher tumor-to-nontumor ratios were achieved, and high ratios were attained much faster. The conventional method produced relatively low tumor-to-nontumor ratios at 24 h; these ratios increased substantially by 72 h, but never (even at 336 hr) approached the levels obtained with the gal-SA method at 29 h for the blood, spleen, kidney and lungs. Table 1 also presents the ratio of the values obtained by the two methods at 24 or 29 h, the time interval that would be most useful for tumor imaging. The advantage of the gal-SA method was greatest for the blood (seven-fold) but was also large for the lungs and kidney (nearly four-fold). For the intestines, the effect of blood clearance was partially offset by the biliary excretion, as noted previously, so the tumor-to-nontumor ratios were worse immediately after clearance, at 29 h. However, by 72 h the tumor-to-intestine ratios obtained by the gal-SA method were comparable to those obtained with the conventional method. For the liver, the ratios were approximately two-fold better with the standard method than with the gal-SA clearance method, but tumor-to-liver ratios were still 2.2:1 at the worst time point tested, which was immediately after blood clearance, and by 72 h, the tumor-to-liver ratio was 4.7:1 ± 0.2.

Similar blood clearance experiments were performed with clearance at 48 or 17 h, instead of the 24 h used in the experiments previously described. Results with clearance at 48 h were very similar to those described previously. Clearance at 17 h resulted in substantially lower tumor uptake, 11.9 ± 2.9 %ID/g just after blood clearance, com-

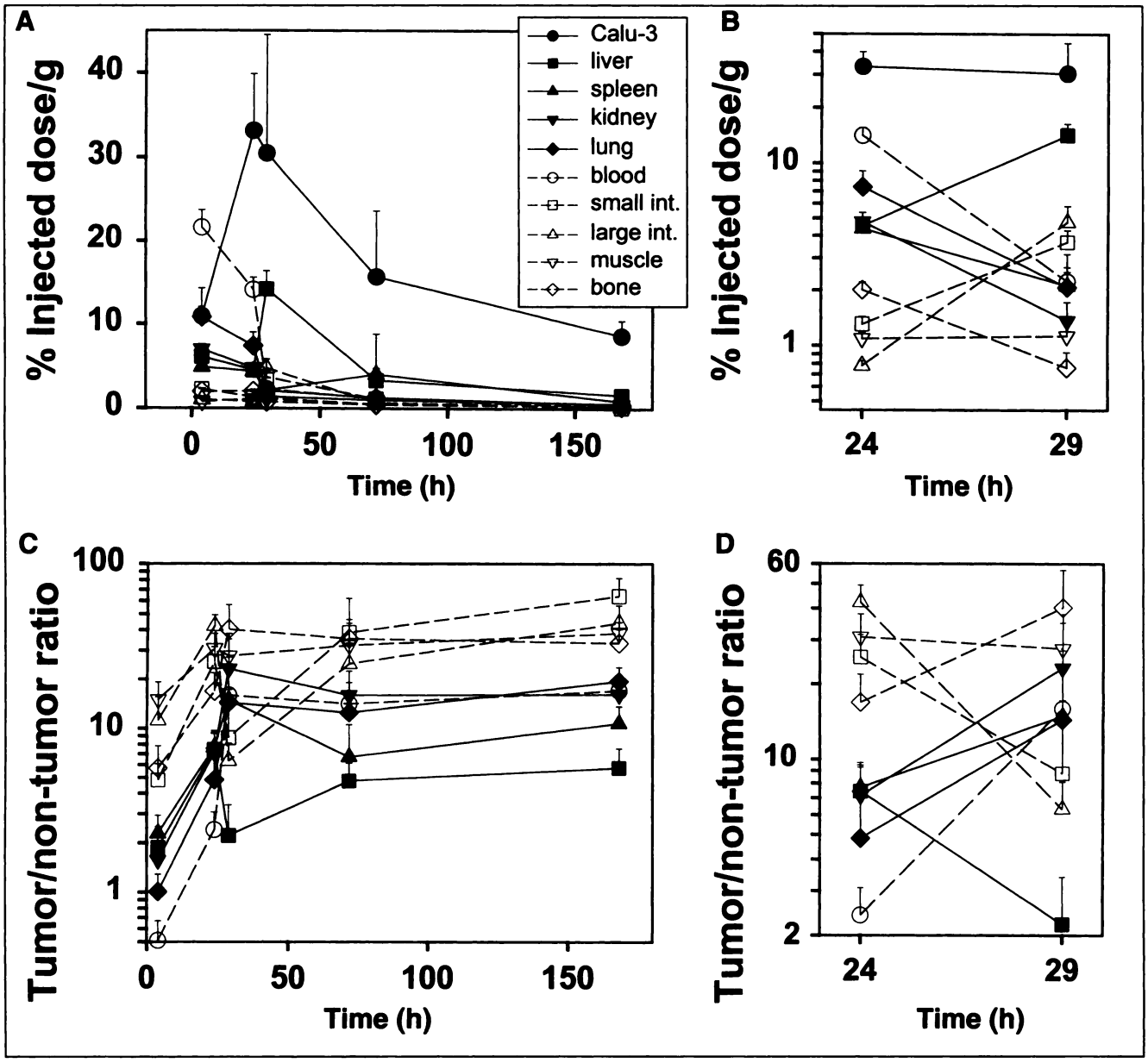

FIGURE 3. Biodistribution of ^{111}In-biotin-RS11 in nude mice bearing Calu-3 lung carcinoma xenografts, with rapid blood clearance induced at 24 h by injection of gal-SA. (A and B) %ID/g; (C and D) tumor-to-nontumor ratios. Blow-up of data at 24 h (B and D), just before clearance, and 29 h, just after clearance is completed (times too close together to be seen clearly in [A] and [C]). Values shown are mean ± SD of 5 mice per group. Mean tumor sizes were 0.13–0.15 g at times 4–29 h, 0.18 g at 72 h and 0.23 g at 168 h. Log scale is used in some graphs simply to improve clarity of figure.

pared with tumor levels of approximately 30 %ID/g when clearance was at 24 or 48 h. These data indicate that tumor penetration and binding was incomplete at 17 h after Ab injection, and that, in this model system, the optimal time for Ab clearance (for imaging purposes) is at 24 h.

To determine whether this approach would be an advantage for radioimmunotherapy (RAIT), radiation dosimetry calculations were performed. It would be expected that, for therapy, earlier blood clearance would be an advantage, because this would reduce the radiation delivered to normal tissues from radioisotope circulating in the blood. These calculations used the ^{111}In biodistribution as a model for the therapeutic isotope ^{90}Y (that binds to the same chelators), which is known to be a close approximation (*24*). Table 2 shows the results of these calculations, in comparison to a standard experiment without induced blood clearance. The blood dose and the liver dose are presented, in addition to the tumor dose. The blood dose provides the best indicator of bone marrow toxicity, which is expected to be the limiting toxicity (*23*). The liver dose is also shown, because the liver-directed clearance could potentially make the liver the dose-limiting organ. Although the liver dose is 2.1-fold higher than the blood dose when clearance is induced at 17 h, it is only 1.4-fold higher when clearance is induced at

TABLE 1
Comparison of Two Methods of RS11 Localization to Calu-3 Tumor Xenografts

Tissue	Tumor-to-nontumor ratio							Ratio at 24–29 h
	^{88}Y-RS11				^{111}In-biotin-RS11 plus gal-SA			
	24 h	72 h	168 h	336 h	29 h	72 h	168 h	^{111}In/^{88}Y
Liver	5.9 ± 1.2	9.4 ± 2.8	8.6 ± 2.1	9.1 ± 2.0	2.2 ± 0.0	4.7 ± 0.2	4.7 ± 1.4	0.37
Spleen	7.6 ± 0.8	11.4 ± 1.2	8.4 ± 2.3	5.3 ± 1.7	14.5 ± 0.6	9.6 ± 4.0	9.4 ± 1.9	1.91
Kidney	5.6 ± 1.2	10.1 ± 1.3	12.1 ± 2.7	12.5 ± 3.6	21.7 ± 2.2	16.8 ± 1.3	14.0 ± 3.0	3.88
Lungs	4.7 ± 0.8	8.0 ± 2.5	7.4 ± 1.4	7.8 ± 1.5	17.4 ± 4.2	17.3 ± 6.8	20.1 ± 0.9	3.70
Blood	2.5 ± 0.7	4.4 ± 1.0	4.3 ± 0.8	8.2 ± 2.5	17.6 ± 2.3	18.8 ± 6.6	19.5 ± 3.5	7.04
Small intestine	18.8 ± 3.8	39.7 ± 5.9	39.2 ± 9.8	59.8 ± 11.0	15.1 ± 8.8	55.7 ± 24.3	57.5 ± 9.1	0.80
Large intestine	24.6 ± 7.3	45.7 ± 12.8	45.9 ± 15.4	74.7 ± 18.3	7.7 ± 2.0	31.8 ± 9.8	42.3 ± 2.5	0.31
Muscle	23.4 ± 7.3	47.3 ± 12.7	44.2 ± 8.0	68.6 ± 19.1	29.3 ± 2.3	33.2 ± 1.4	33.9 ± 5.9	1.25

gal-SA = galactosylated streptavidin.

^{88}Y-RS11 data were from standard biodistribution experiment, without any manipulation of blood clearance rate (method 1); it is taken from previous publication (*11*) and is used here for comparative purposes. For ^{111}In-biotin-RS11 plus gal-SA data, blood clearance was induced by injection of gal-SA at 24 h, and clearance was essentially complete at 29 h (method 2). Although different radiometal was used, there is no significant difference between biodistribution of ^{88}Y or ^{111}In labels, with chelator used, except for slight difference in bone uptake, as noted in text. Values shown for ^{88}Y-RS11 experiment are mean ± SD of 4–5 mice per group; for ^{111}In-biotin-RS11 plus gal-SA experiment, they are mean ± SD of two experiments, each having 5 mice per group. Differences between two methods are statistically significant ($P < 0.001$) for blood, lungs, kidney and spleen for all time points. Last column presents ratios of (tumor-to-nontumor ratio by method 2 at 29 h)/(tumor-to-nontumor ratio by method 1 at 24 h) to facilitate comparison.

24 h, which appears to be the optimal time for RAIT. Thus, as a result of the greater radiation resistance of the liver relative to the bone marrow, the bone marrow would still be the dose-limiting organ. The ratio, tumor dose-to-blood dose, included in the table, is thus a reasonable measure of specific therapeutic effect. As shown, the use of the gal-SA method does not appear to provide a substantial advantage for therapy. For comparative purposes, Table 2 also includes dosimetry calculations for ^{131}I-DLT-labeled RS11 (*11*), which show that the simple injection of this residualizing iodine label appears to provide the highest tumor-to-blood dose ratio.

To establish the generality of the blood clearance method, similar experiments were performed with a different Ab and tumor cell line, and the results are shown in Figure 4. In this study, the colon carcinoma LS174T, Ab MN-14, and clearance at 24 h were used. One advantage of this experimental model is that it has been extensively used with a variety of radiolabels and Ab fragments, therefore allowing comparison with historical data. As shown, blood clearance was slightly more effective than in the RS11 experiments, with a reduction from 12.7 ± 2.3 %ID/g at 24 h to 0.7 ± 0.4 %ID/g at 29 h, an 18-fold decrease, resulting in a tumor-to-blood ratio of 31.0 ± 11.4 at 29 h. Very similar to the results described previously with Ab RS11, the efficient blood clearance resulted in high tumor-to-nontumor ratios at 29 h for all normal tissues, except the liver and the intestines. Thus, the tumor-to-kidney ratios increased from 2.9% ± 1.7% at 24 h to 11.3% ± 4.6% at 29 h, the tumor-to-lung ratio increased from 2.7% ± 1.6% to 16.8% ± 6.8%, and the tumor-to-spleen and tumor-to-bone ratios increased to a somewhat lesser extent. In this experiment, unlike the RS11 experiment shown in Figure 2, the tumor-to-muscle ratio was substantially increased by blood clearance, from 11.5% ± 7.4% to 26.9% ± 9.6%. The tumor-to-nontumor ratios for the intestines decreased from 24–29 h, but then increased to high levels at 72 h. The tumor-to-liver ratio remained slightly >1.0 at time points out to 3 d; at day 7, the tumor-to-liver ratio decreased to 0.56, indicating that the label was retained somewhat better by the liver than by the tumor. The liver uptake both before and after clearance was considerably greater in the MN-14 experiment than in the RS11 experiments. Because this difference in liver uptake was present at 24 h, before the clearing agent was injected, it was not a result of the clearing protocol itself. The amount of activity in the liver at 24 h was 9.2% ± 2.8% in the LS174T experiments and 4.5% ± 0.3% in the Calu-3 experiment, and this difference (approximately 5%) was maintained for the 7-d duration of the experiment.

TABLE 2
Dosimetry Calculations for Antibody RS11 Localizing to Calu-3 Xenografts

Experiment	cGy/MBq injected			Tumor-to-blood ratio
	Tumor	Blood	Liver	
Standard ^{90}Y	774	271	150	2.9
Standard ^{131}I-DLT	675	93	103	7.3
Clearance at 17 h	249	110	229	2.3
Clearance at 24 h	413	141	193	2.9
Clearance at 48 h	437	167	141	2.6

All calculations are for ^{90}Y, except as noted, but are based on experiments performed with ^{111}In. Standard experiment denotes simple injection of antibody, whereas clearance experiments denote blood clearance induced with galactosylated streptavidin at time indicated.

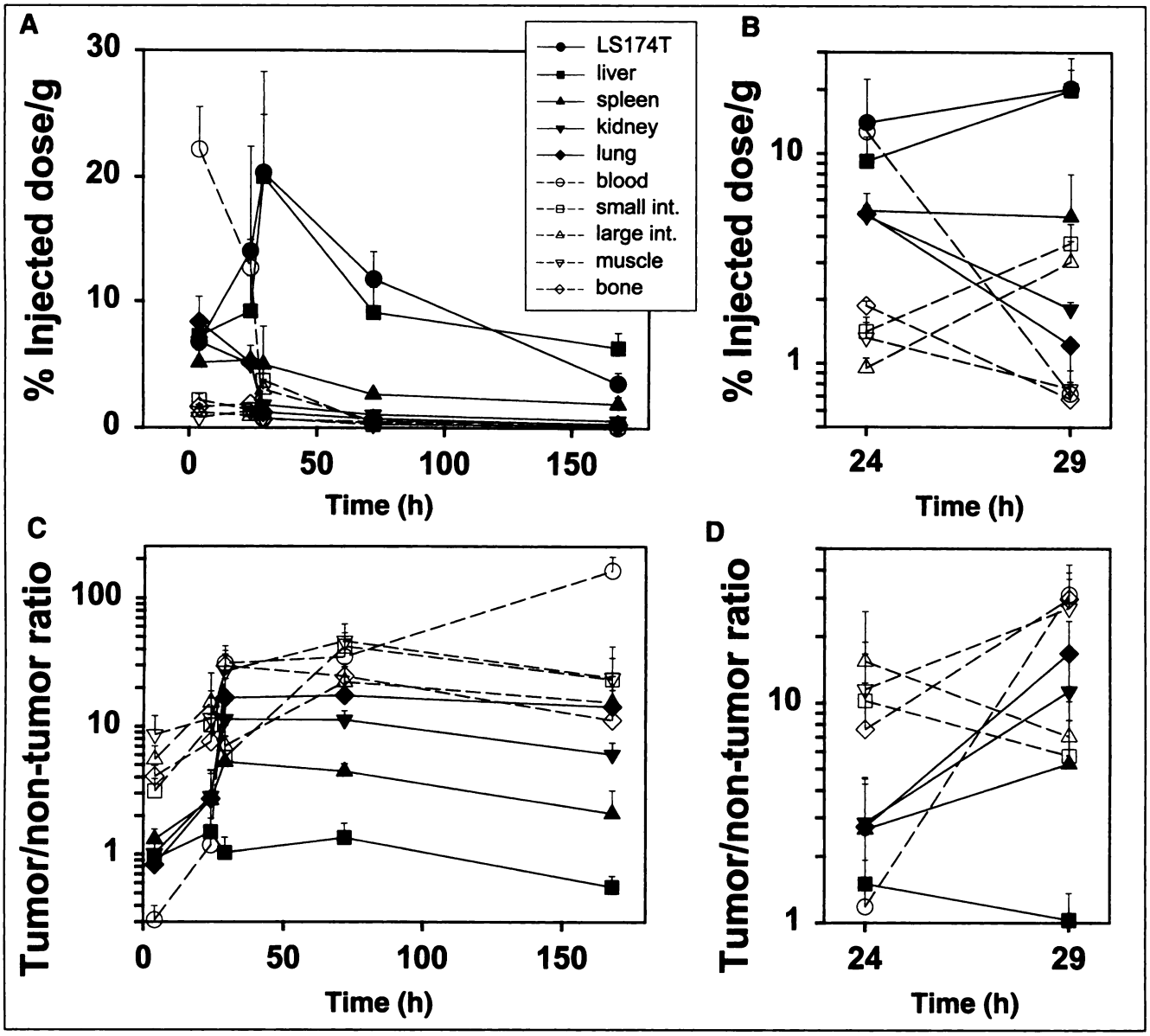

FIGURE 4. Biodistribution of ^{111}In-biotin-MN-14 in nude mice bearing LS174T colon carcinoma xenografts, with rapid blood clearance induced at 24 h by injection of gal-SA. (A and B) %ID/g; (C and D) tumor-to-nontumor ratios. Blow-up of data at 24 h (B and D), just before clearance, and 29 h, just after clearance is completed (times too close together to be seen clearly in [A] and [C]). Values shown are mean ± SD of 5 mice per group. Mean tumor sizes were 0.40–0.47 g at times 4–72 h and 1.28 g at 168 h. Log scale is used in some graphs simply to improve clarity of figure.

Because tumor counts per minute decreased during this period, the 5% increment in the liver had a greater effect on the tumor-to-liver ratio at later time points. Radiation dosimetry calculations were also performed for this experiment, for a ^{90}Y label. The ratio of the cGy dose for tumor-to-blood was 1.39, which is somewhat lower than the values obtained with a simple injection of Ab (albeit with an ^{88}Y label rather than ^{111}In) (GL Griffiths and DM Goldenberg, unpublished data, July 1993).

DISCUSSION

The strategy described herein produced very high tumor-to-nontumor ratios 1 d after Ab injection. We believe that this approach is potentially widely applicable for imaging purposes and that generally similar strategies can be applied with other protein imaging agents. Many other approaches to induce blood clearance, for the same purpose, are also under investigation (*5–7,16,25–28*). Although it is difficult to compare the results with those described here because of the differences in the tumor target, the Ab and other parameters, none of the previously described methods has the theoretical advantages of the gal-SA clearance method. Although some liver accumulation of isotope did occur with the gal-SA method, the level was not very high, and tumor-to-liver ratios remained >1.0. The transient uptake in the intestines, due to biliary excretion, could be reduced by

emptying the intestinal tract, which can be achieved in various ways. Streptavidin, either alone or in various conjugates (*28*), has been injected into patients, so the method proposed here can probably be applied, in a relatively straightforward fashion, to the clinic.

The effect of gal-SA clearance is most clearly seen by comparing values obtained just before clearance with those just after clearance, which was 5 h later. These two time points would be basically the same in the absence of induced blood clearance, and the values obtained before clearance therefore provide the values that would be obtained in a simple Ab biodistribution experiment. In addition, for comparative purposes, we have provided in Table 1 historical data with ^{88}Y-benzyl-DTPA-RS11 and the Calu-3 tumor (the difference in the radiometal is not significant for our current purpose, as previously discussed). These data show that, although the tumor-to-blood ratios did increase with time in a simple biodistribution experiment, they never reached the values obtained at 29 h with gal-SA clearance. Although we have not included similar data with the LS174T model system, the general pattern of results was very similar. In particular, the tumor-to-blood ratio, 31.0 in these experiments, was only 2.2 to 4.3 at 24 h in conventional biodistribution experiments (GL Griffiths and DM Goldenberg, unpublished data, July, 1993), and even by day 7 did not exceed 14.2.

Our experiments used two Ab/target cell combinations to establish the generality of the results, but an important difference between these two models should be noted. Although RS11 biodistribution has been shown to benefit markedly from the use of a residualizing radiolabel (*11*), because the Ab is internalized and catabolized at a substantial rate, this is not the case for anti-CEA (MN-14). With this Ab, the residualizing label ^{111}In has little advantage over the nonresidualizing label conventional ^{125}I (*24*); presumably because there is little internalization of the Ab. Thus, this model would not take advantage of one of the features of the method described, the use of a residualizing radiolabel. However, it was selected for these experiments because of the extensive published work with this model, in which Fab′ or F(ab′)$_2$ fragments labeled with ^{99m}Tc were used in Ab biodistribution experiments (*4*). In any case, these experiments with MN-14 demonstrate that, even for Abs that are not substantially internalized, the gal-SA clearance method produces high tumor-to-nontumor ratios.

The blood clearance of MN-14 by gal-SA was considerably more efficient than with RS11. This cannot be explained, but might be attributed to small impurities or heterogeneity in the RS11 Ab preparation. We note that Ab MJ37, used in Figure 2, was also cleared somewhat more efficiently than RS11, with <1.0 %ID/g blood remaining 5 h after clearance. The markedly greater liver uptake of MN-14 compared with RS11, which occurred before clearance was induced and which persisted throughout the course of the experiments, can be most readily interpreted as resulting from uptake of Ab-antigen complexes by Kupffer cells in the liver. Because the Kupffer cells cannot excrete the radiolabel into bile, as demonstrated in previous experiments (*16*), the label would be retained for long periods within these cells. In fact, Beatty et al. (*29*), using the same LS174T tumor, demonstrated that anti-CEA Abs localized significantly to the liver of tumor-bearing nude mice because of the formation of immune complexes (*29*).

It has been argued that ^{99m}Tc-labeled Ab fragments are the most suitable tumor imaging agents (*1,3,4*). Localization of ^{99m}Tc-Ab fragments of MN-14 to LS174T tumors was determined previously (*4*). On the basis of the data presented here, the tumor-to-nontumor ratios produced by gal-SA clearance were markedly higher than those obtained with either Fab′ or F(ab′)$_2$ for the blood, kidney, lungs and bone, for time points of 24–29 h. The advantage was due both to higher tumor uptake and to lower uptake in the normal tissues. Only the liver displayed a lower ratio. Because the liver is an important metastatic site for colon carcinoma, it may be necessary in some cases to select the imaging method to be used based on the organ of major interest.

The studies of Gautherot et al. (*26*) and Janevik-Ivanovska et al. (*27*) are relevant to this work, because they used the same tumor model, LS174T, and the same target antigen, CEA, as used here, although with a different Ab. These authors used a pretargeting method, with bispecific Abs and bivalent radiolabeled haptens. Their tumor-to-blood ratios were lower than those obtained here at day 1, whereas at later time points the ratios were generally similar to those obtained here. In general, it should be noted that each method has certain disadvantages, such as kidney uptake with pretargeting and liver uptake with the gal-SA clearance method. One difference between the gal-SA clearance method and many of the competing methods is that the former results in higher absolute values of percentage of the injected dose per gram of tumor. Although it is considered that the tumor-to-nontumor ratio is the critical parameter in tumor imaging, it must be true at some level that the absolute uptake in the tumor can be a significant factor, particularly in attempting to detect very small tumors, or tumors having low antigen expression.

The first use of a galactosylated clearing agent was by Bagshawe (*30*) and others (*31*), who used a galactosylated second Ab. These reports demonstrated that the clearing agent remained in the circulation long enough to bind to the labeled molecules, which was not obvious, considering that uptake by the ASGP-r is complete within minutes, probably in one or a few passes through the liver. The first use of gal-SA in conjunction with biotinylated Abs was by Marshall et al. (*9*), who also demonstrated that such clearance was through hepatocytes, as expected. This clearing agent probably has a significant advantage over the use of a galactosylated second Ab: because a second Ab forms immune complexes, it can potentially bind to both Fc receptors, on Kupffer cells and macrophages, as well as to the ASGP-r on hepatocytes. Thus, it may not provide as

"clean" a delivery to hepatocytes. However, this possibility is only speculative at this time.

The advantage of intraperitoneal over intravenous injection of the clearing agent was described by Marshall et al. (9) and confirmed here. This can be attributed to the fact that a considerable fraction of the Ab is in interstitial fluid at the time of injecting the clearing agent, and therefore will not be bound by gal-SA injected intravenously before the rapid removal of this clearing agent from the blood. This Ab will gradually re-equilibrate from interstitial fluid to blood. In contrast, with an intraperitoneal injection of gal-SA, the Ab moves more gradually from the peritoneal cavity to blood, which effectively means that the clearing agent will be present in the blood for a longer period. Similarly, the second injection of the clearing agent is effective probably because it removes Ab that was in interstitial fluid at the time of the first injection but has since been transferred from interstitial fluid to blood.

By performing dosimetry calculations, we have attempted to predict whether this approach would be advantageous for RAIT. It is likely that the conditions optimal for imaging will not be the same as those optimal for therapy. More specifically, imaging requires the highest possible tumor-to-nontumor ratio at a single time point, whereas therapy depends on the area under the curve of radioactivity versus time. Therefore, it would be expected that optimal imaging would be achieved by clearance induction as late as possible, depending on the half-life of the isotope used, to allow maximal Ab uptake in the tumor. In contrast, optimal therapeutic ratios would be achieved by earlier clearance induction, to reduce the nonspecific radiation dose delivered by Ab circulating in the blood. Accordingly, experiments were performed with clearance at 17 h, which was considered to be the earliest time at which substantial Ab uptake in the tumor would occur, as well as at later time points. However, even with this early clearance, or with later clearance, there is little or no dosimetry advantage of the gal-SA clearance method compared with the simple use of a radiolabeled Ab, due primarily to decreased tumor uptake.

CONCLUSION

By selecting an Ab radiolabel that is trapped within tumor cells but is excreted from hepatocytes into bile, and by using a clearance method that delivers the Ab to hepatocytes, high tumor-to-nontumor ratios were obtained 1 d after injection of the radiolabeled Ab. The radiolabel was ^{111}In-benzyl-DTPA, and the clearing agent was gal-SA, used in conjunction with biotinylated Abs. For most organs, the tumor-to-nontumor ratios obtained were considerably higher than those that have been obtained by other approaches using the same tumor xenograft models and the same Abs. Uptake in the liver was substantial, but tumor-to-liver ratios remained >1 as a result of biliary excretion. Transient uptake in the intestines was due to biliary excretion. This method may be widely applicable to the imaging of tumors and other diseases with Abs or other protein targeting agents.

ACKNOWLEDGMENTS

We are grateful to Drs. Gary L. Griffiths, Habibe Karacay and Robert M. Sharkey for collaborative assistance, to Philip Andrews, Tom Jackson and Tony Zarcone for assistance with radiolabeling, and to Susan Chen for assaying Ab immunoreactivity and for tissue culture support. This work was supported in part by U.S. Public Health Service National Institutes of Health grants CA63624, CA60039 and CA39841. Sagar Patel was supported by the UPTAM program of the Stevens Institute of Technology.

REFERENCES

1. Goldenberg DM. Monoclonal antibodies in cancer detection and therapy. *Am J Med.* 1993;94:297–312.
2. Waldmann TA, Strober W. Metabolism of immunoglobulins. *Prog Allergy.* 1969;13:1–110.
3. Moffatt F, Pinsky CM, Hammerschaimb L, et al. Clinical utility of external immunoscintigraphy with the IMMU-4 ^{99m}Tc Fab′ antibody fragment (CEA-Scan TM: arcitumomab) in patients undergoing surgery for carcinoma of the colon and rectum: results of a pivotal, phase III trial. *J Clin Oncol.* 1996;14:2295–2305.
4. Govindan SV, Goldenberg DM, Grebenau RC, Hansen HJ, Griffiths GL. Thiolations, ^{99m}Tc labelings, and animal in vivo biodistributions of divalent monoclonal antibody fragments. *Bioconjugate Chem.* 1996;7:290–297.
5. Chen JQ, Strand S-E, Tennvall J, Lindgren L, Hindorf C, Sjogren H-O. Extracorporeal immunoadsorption compared to avidin chase: enhancement of tumor-to-normal tissue ratio of biotinylated rhenium-188-chimeric BR96. *J Nucl Med.* 1997;38:1934–1939.
6. Sharkey RM, Boerman OC, Natale A, et al. Enhanced clearance of radiolabeled murine monoclonal antibody by a syngeneic anti-idiotype antibody in tumor-bearing nude mice. *Int J Cancer.* 1992;51:266–273.
7. Pedley RB, Dale R, Boden JA, Begent RHJ, Keep PA, Green AJ. The effect of second antibody clearance on the distribution and dosimetry of radiolabelled anti-CEA antibody in a human colonic tumor xenograft model. *Int J Cancer.* 1989;43:713–718.
8. Ong GL, Ettenson D, Sharkey RM, et al. Galactose-conjugated antibodies in cancer therapy: properties and principles of action. *Cancer Res.* 1991;51:1619–1626.
9. Marshall D, Pedley RB, Melton RG, Boden JA, Boden R, Begent RHJ. Galactosylated streptavidin for improved clearance of biotinylated intact and F(ab′)$_2$ fragments of an anti-tumour antibody. *Br J Cancer* 1995;71:18–24.
10. Duncan JR, Welch MJ. Intracellular metabolism of indium-111-DTPA-labeled receptor targeted proteins. *J Nucl Med.* 1993;34:1728–1738.
11. Stein R, Goldenberg DM, Thorpe SR, Basu A, Mattes MJ. Effects of radiolabeling monoclonal antibodies with a residualizing iodine radiolabel on the accretion of radioistope in tumors. *Cancer Res.* 1995;55:3132–3139.
12. Stein R, Goldenberg DM, Thorpe SR, Mattes MJ. Advantage of a residualizing iodine radiolabel for radioimmunotherapy of xenografts of human non-small-cell carcinoma of the lung. *J Nucl Med.* 1997;38:391–395.
13. Renaud G, Hamilton RL, Havel RJ. Hepatic metabolism of colloidal gold-low-density lipoprotein complexes in the rat: evidence for bulk excretion of lysosomal contents into bile. *Hepatology.* 1989;9:380–392.
14. Kornfeld S, Mellman I. The biogenesis of lysosomes. *Ann Rev Cell Biol.* 1989;5:483–525.
15. Arano Y, Mukai T, Uezono T, et al. A biological method to evaluate bifunctional chelating agents to label antibodies with metallic radionuclides. *J Nucl Med.* 1994;35:890–898.
16. Stein R, Goldenberg DM, Ong GL, Thorpe ST, Mattes MJ. Manipulation of blood clearance to optimize delivery of residualizing label-antibody conjugates to tumor cells in vivo. *J Nucl Med.* 1997;38:1392–1400.
17. de Leij L, Helrich W, Stein R, Mattes MJ. SCLC-cluster 2 antibodies detect the pancarcinoma/epithelial glycoprotein EGP-2. *Int J Cancer.* 1994;(suppl 8): 60–63.
18. Ong GL, Mattes MJ. Penetration and binding of antibodies in experimental and solid tumors. *Cancer Res.* 1989;49:4264–4273.
19. Mattes MJ. Binding parameters of antibodies reacting with multivalent antigens: functional affinity or pseudo-affinity. *J Immunol Meth.* 1997;202:97–101.
20. Mattes MJ. Biodistribution of antibodies after intraperitoneal or intravenous injection and effect of carbohydrate modifications. *J Natl Cancer Inst.* 1987;79: 855–863.

21. Hansen HJ, Goldenberg DM, Newman ES, Grebenau R, Sharkey RM. Characterization of second-generation monoclonal antibodies against carcinoembryonic antigen. *Cancer.* 1993;71:3478–3485.
22. Siegel JA, Stabin MG. Absorbed fractions for electrons and beta particles in spheres of various sizes. *J Nucl Med.* 1994;35:152–156.
23. Sharkey RM, Blumenthal RD, Behr TM, et al. Selection of radioimmunoconjugates for the therapy of well-established or micrometastatic colon carcinoma. *Int J Cancer.* 1997;72:477–485.
24. Sharkey RM, Motta-Hennessy C, Pawlyk D, Siegal JA, Goldenberg DM. Biodistribution and radiation dose estimates for yttrium- and iodine-labeled monoclonal antibody IgG and fragments in nude mice bearing human colonic tumor xenografts. *Cancer Res.* 1990;50:2330–2336.
25. Sharkey RM, Karacay H, Griffiths GL, et al. Development of a streptavidin-anti-carcinoembryonic antigen antibody, radiolabeled biotin pretargeting method for radioimmunotherapy of colorectal cancer. Studies in a human colon cancer xenograft model. *Bioconjug Chem.* 1997;8:595–604.
26. Gautherot E, Bouhou J, Le Doussal J-M, et al. Therapy for colon carcinoma xenografts with bispecific antibody-targeted, iodine-131-labeled bivalent hapten. *Cancer.* 1997;80:2618–2623.
27. Janevik-Ivanovska E, Gautherot E, de Boisferon MH, et al. Bivalent hapten-bearing peptides designed for iodine-131 pretargeted radioimmunotherapy. *Bioconjug Chem.* 1997;8:526–533.
28. Paganelli G, Magnani P, Siccardi AG, eds. *Clinical Applications of the Avidin-Biotin System for Tumor Targeting.* Boca Raton, FL: CRC Press; 1995.
29. Beatty JD, Beatty BG, O'Conner-Tressel M, Do T, Paxton RJ. Mechanisms of tissue uptake and metabolism of radiolabeled antibody: role of antigen:antibody complex formation. *Cancer Res.* 1990;50:840S–845S.
30. Bagshawe KD. Towards generating cytotoxic agents at cancer sites. *Br J Cancer.* 1989;60:275–281.
31. Rogers GT, Burke PJ, Sharma SK, Koodie R, Boden JA. Plasma clearance of an antibody-enzyme conjugate in ADEPT by monoclonal anti-enzyme: its effect on prodrug activation *in vivo*. *Br J Cancer.* 1995;72:1357–1363.